Evidence for a strongly bound kaonic system K^-ppn in the ^{4}He(stopped K^-,n) reaction

M. Iwasaki [a,b], T. Suzuki [c], H. Bhang [d], G. Franklin [e], K. Gomikawa [c], R.S. Hayano [c], T. Hayashi [b,*], K. Ishikawa [b], S. Ishimoto [f], K. Itahashi [a], T. Katayama [b], Y. Kondo [b], Y. Matsuda [a], T. Nakamura [b], S. Okada [b], H. Outa [f,**], B. Quinn [e], M. Sato [b], M. Shindo [c], H. So [d], T. Sugimoto [b], P. Strasser [a], K. Suzuki [c,***], S. Suzuki [f], D. Tomono [b], A.M. Vinodkumar [b], E. Widmann [c], T. Yamazaki [a], T. Yoneyama [b]

[a] *RIKEN Wako Institue, RIKEN (The Institute of Physical and Chemical Research), Wako-shi, Saitama, 351-0198, Japan*

[b] *Department of Physics, Tokyo Institute of Technology, Ookayama, Meguro-ku, Tokyo 152-8551, Japan*

[c] *Department of Physics, University of Tokyo, Hongo, Bunko-ku, Tokyo 113-0033, Japan*

[d] *Department of Physics, Seoul National University, Shikkim-dong, Kwanak-gu, 151-742, Korea*

[e] *Department of Physics, Carnegie Mellon University, Pittsburgh, PA 15213, USA*

[f] *IPNS, KEK (High Energy Acceralator Research Organization), Ooho, Tsukuba-shi, Ibaraki 305-0801, Japan*

Abstract

We measured a neutron energy spectrum by means of time-of-flight (TOF) from the $^4\mathrm{He}(K^-_{stopped}, n)$ reaction by stopping negative kaons in a super-fluid helium target. A distinct peak was observed in the neutron spectrum, indicating the formation of a strongly bound kaonic system, K^-ppn, with the binding energy and width, $B_{Kppn} = 173 \pm 4$ MeV and $\Gamma_{Kppn} \lesssim 25$ MeV, respectively.

Key words:
PACS: 11.30.Rd 13.75.Jz 21.10.Dr 25.75.Nq 26.60.+c

Since the so-called "kaonic hydrogen puzzle" was solved by the kaonic hydrogen (KpX) experiment at KEK [1], the KN interaction was established to be strongly attractive in the isospin $(I) = 0$ channel, so that $\Lambda(1405)$ can be interpreted as a bound state between K^- and proton. Recently, Akaishi and Yamazaki performed a coupled-channel calculation to empirically determine the KN interaction strengths and their range using the kaonic hydrogen and the KN scattering data, as well as the energy and width of $\Lambda(1405)$. With their KN interaction parameters, they predicted that strongly bound kaonic states with narrow widths can be formed in light nuclei [2]. Especially, the $T = 0$ K^-ppn (or $\overline{K}^0pnn$) system is predicted to be a strongly bound state with a total binding energy $B_K = 115$ MeV (measured from $K^- + p + p + n$; $M = 3309.8$ MeV) and a width $\Gamma_K = \Gamma_N + \Gamma_{NN} = 20 + 12 = 32$ MeV, where Γ_N and Γ_{NN} are for the one-nucleon ($\pi\Lambda NN$) and two-nucleon (ΛNN or ΣNN) decay channels respectively.

According to their prediction the K$^-$-p interaction is so strong as to shrink the nuclei and to form extraordinarily dense systems with a central nucleon density of $\sim$5 ρ_0. A further study using the anti-symmetrized molecular dynamics method (AMD) by Dote *et al.* predicted even higher central density values of 8$\sim$10 ρ_0 [3]. If this is the case, and such bound states are found, we may be able to study dense and cold nuclear systems in which chiral symmetry is expected to be restored, and quarks may be deconfined [4]. Hence, experimental studies of such states are of great importance, and may provide rich information to understand the dynamics of the neutron and/or strange star [5].

In the present experiment we adopted the $(K^-_{stopped}, n)$ reaction on ^{4}He. If the K^-ppn state is formed, a mono-energetic "Auger" neutron should be produced via the

$$K^- +^4 \mathrm{He} \rightarrow K^-ppn + n \tag{1}$$

reaction. The mass of K^-ppn system can be determined from the kinetic energy of the emitted neutron [6].

The experiment was carried out at the KEK 12 GeV proton synchrotron. We stopped negative kaons in a super-fluid helium target, and applied the TOF method to measure the energy of the neutron, by using plastic scintillation counter (NC) matrices of about 2 m^3, located 2 m from the helium target (Fig. 1). We adopted a target cell of 1.87 g/cm^2 thick with window thickness of 75 μm, operated at 20 torr. The target cell was covered by a 0.2 mm-thick aluminum heat shield and a 0.9 mm-thick CFRP vacuum jacket. The high thermal conductivity of super-fluid helium allowed us to keep major cryogenic

* Present address: Dept. of Legal Med., Osaka Univ.
** Present address: Wako Institue, RIKEN
*** Present address: GSI
Email address: muon@riken.go.jp (M. Iwasaki).

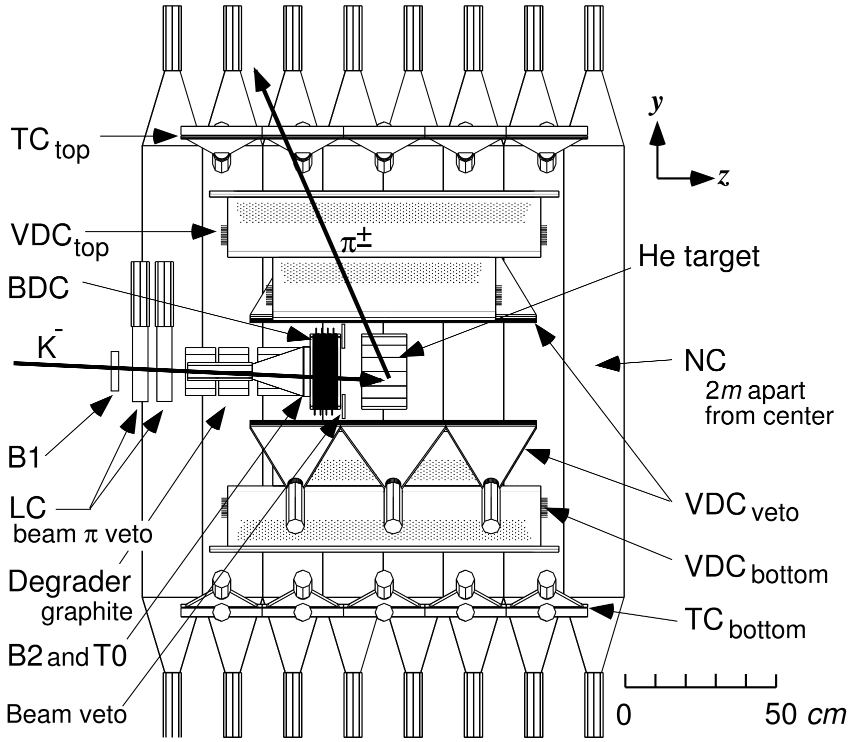

Fig. 1. A schematic cross-sectional view of the setup, showing Lucite Čerenkov counters LC, a beam counters B1, B2 and T0, beam drift chamber BDC, a helium target, neutron counters NC (placed 2 m behind the target), drift chambers VDC_{up} and VDC_{down} and two layers of TC counters.

elements away from the target cell.

The incoming kaon was registered by beam line counters (B1, B2 and T0) and tracked by high-rate drift chambers (BDC). As shown in Fig. 1, we also required that a charged particle is emitted from the target region, which we tracked by large-area drift chambers (VDC) placed above and below the helium target. Behind the VDCs, we placed two slabs of plastic counters (TC's) of the thickness of 6 and 30 mm. With these counters, we could distinguish $\pi^{\pm}$'s from protons, and could also roughly measure their momenta.

The reaction (or neutron-production) point was determined by the vertex between the trajectory of an incoming kaon and that of an outgoing charged particle. The resolution of the reaction points/vertex was $\sim$5 mm (σ), which is predominantly determined by kaon multiple scattering in the target helium. The kaon reaction at-rest in the target volume was selected (purity $> 95\%$) by using the correlation between the pulse height of T0 and the vertex position (the range in the helium target). The reaction (neutron TOF start) timing was calculated from the T0 timing and the kaon range in the target. Absolute time calibration of NC was performed by electromagnetic showers produced in iron-plate converters, placed between NC veto counters and NC itself. The overall TOF resolution of $\Delta(1/\beta) = 0.04(\sigma)$ was achieved.

In addition to the "Auger" neutron, many other processes such as hyperon decays, kaon two-nucleon absorption processes, *etc.*, contribute to the neutron spectrum. Let us first demonstrate that we can obtain a rather simple spectrum by selecting slow ($\lesssim$ 100 MeV/c) pions in coincidence with a neutron (see Fig. 1).

Fig. 2 (top) shows the obtained neutron momentum spectrum. The biggest structure exists from ~200 to ~400 MeV/c. This comes mainly from the π^- two-nucleon absorption reaction (occurring in or around of the target) $\pi^- NN \rightarrow NN$ (denoted as $n_{\pi NN}$) [6]. The lower momentum cut-off at ~ 200 MeV/c is due to the energy threshold of NC (threshold =10 MeV electron equivalent (MeVee)). The spike at ~ 100 MeV/c is due to accidental background.

The spectrum has a "plateau" structure beyond ~500 MeV/c. This comes from the kaon two-nucleon absorption and its chain;

$$K^- NN \rightarrow \mathit{\Lambda} n_{\Lambda \mathrm{N}} \quad \text{and} \quad \mathit{\Lambda} \rightarrow \pi^- p, \tag{2}$$

where $n_{\Lambda \mathrm{N}}$ is the neutron from two-nucleon kaon absorption reaction. Note that pions from Σ decays do not contribute when we select low-momentum pions [7]. We can also exclude contributions from other reaction channels such as hyperon quasi-free (QF: $K^- N \rightarrow \pi Y$), because there is no energy left to produce a neutron in this momentum region.

The spectrum shape of $n_{\Lambda \mathrm{N}}$ is dominantly determined by the three-body phase space and the nuclear form factor, and is very broad as shown in the figure. It has the maximum momentum of ~700 MeV/c, and forms a flat-"plateau" below ~600 MeV/c.

The lower momentum background in "slow-pi" is due to a QF-Σ production followed by a $\Sigma - \Lambda$ conversion inside the nucleus;

$$K^- N \rightarrow \mathit{\Sigma}^{\pm} \pi^{\mp}, \; \mathit{\Sigma}^{\pm} N \rightarrow \mathit{\Lambda} n_{\Sigma \Lambda} \text{ and } \mathit{\Lambda} \rightarrow \pi^0 n_{\Lambda \mathrm{D}}, \tag{3}$$

where $n_{\Sigma \Lambda}$ and $n_{\Lambda \mathrm{D}}$ respectively denote the neutron from $\Sigma - \Lambda$ conversion and that from the $\mathit{\Lambda}$ decay.

Thus, the high-momentum neutrons observed in coincidence with slow pions in Fig. 2 are due to the reaction (2). Then, there must be a clear back-to-back correlation between the neutron and the Λ directions. In order to quantify this, we introduce a vector-at-closest-approach ($\mathbf{v}_{\mathrm{CA}}$), which is the vector from the kaon trajectory to that of the charged pion at the minimum distance. In addition, we define a scalar product $\mathbf{v}_{\mathrm{CA}} \cdot \hat{\mathbf{v}}_n$, where $\hat{\mathbf{v}}_n$ is the normalized vector of detected neutron motion (see Fig. 3).

The back-to-back correlation should be reflected in the *negative* value of $\mathbf{v}_{\mathrm{CA}} \cdot$

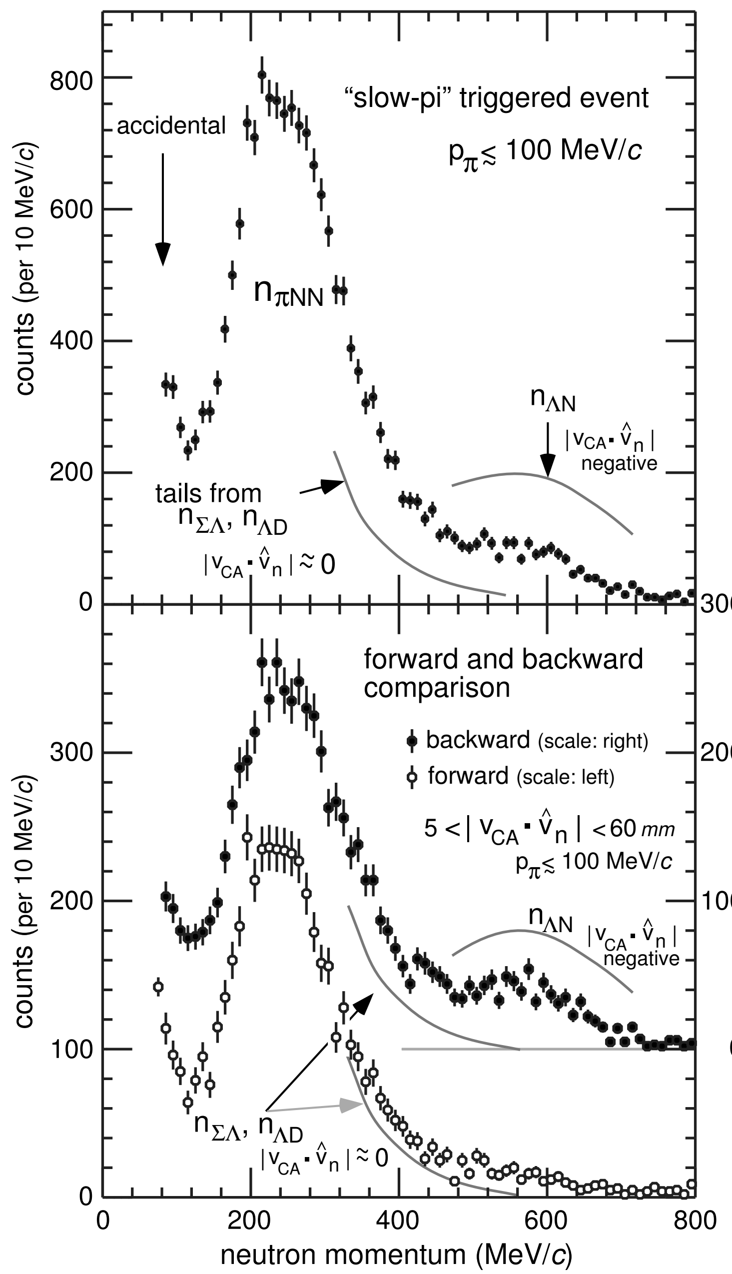

Fig. 2. The neutron momentum spectrum measured in coincidence with a low momentum pion $p_\pi \lesssim 100$ MeV/c (top). The "backward" events (filled circles) ($-60mm < \mathbf{v}_{\rm CA} \cdot \hat{\mathbf{v}}_n < -5mm$) and "forward" events (open circles) ($5mm < \mathbf{v}_{\rm CA} \cdot \hat{\mathbf{v}}_n < 60mm$) are selected and compared (bottom). The rough shape of the spectrum is shown in curve. The curve is to indicate rough spectrum shape, which is obtained simple spline fit and displaced vertically.

$\hat{\mathbf{v}}_n$ (backward). As shown in Fig. 2 (bottom), this is indeed the case. The "plateau" appears only in the *backward* spectrum as expected. We have thus clearly understood the "slow-pi" event set.

What then happens, if we set "fast-pi" event window to select Σ decay (135

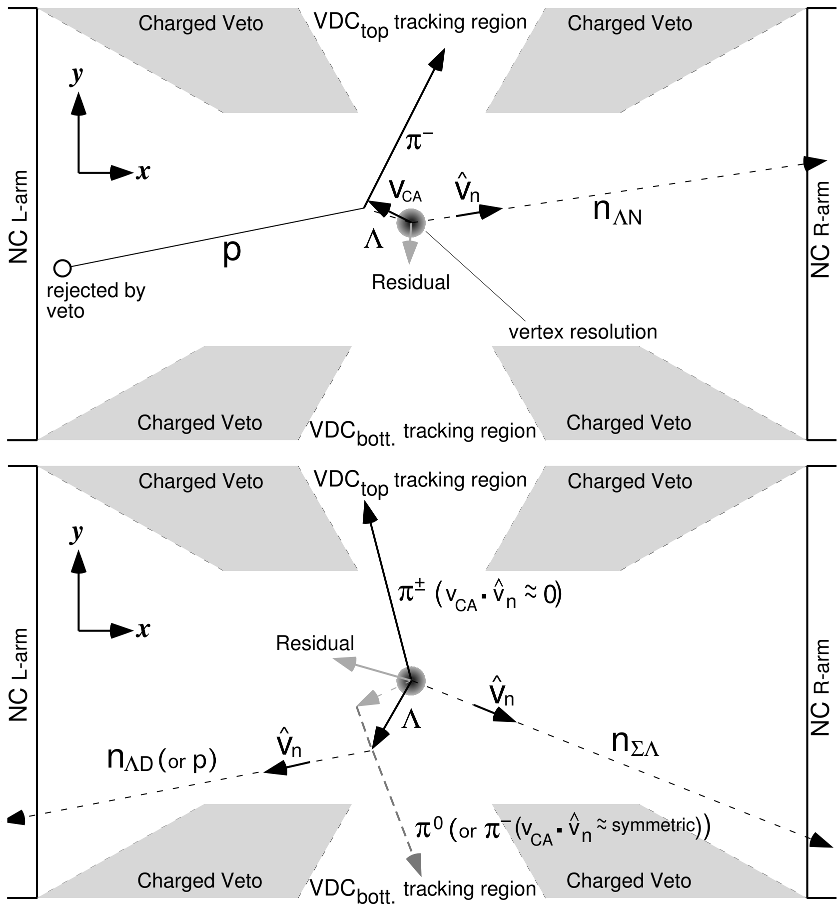

Fig. 3. Top: the definition of $\mathbf{v}_{\mathrm{CA}}$. As an example, a $KNN \rightarrow \Lambda N$ event topology is shown. A kaon comes from behind the paper, and a pion is tracked by the VDC. A vector from the kaon track to the pion track at their closest approach is $\mathbf{v}_{\mathrm{CA}}$. When we require a high momentum neutron hit in the NC, then the $\mathbf{v}_{\mathrm{CA}}$ should be a good approximation of the hyperon motion, and thus $\mathbf{v}_{\mathrm{CA}} \cdot \hat{\mathbf{v}}_n$ gives the hyperon momentum vector and its distance relative to the neutron momentum vector. A scalar product $\mathbf{v}_{\mathrm{CA}} \cdot \hat{\mathbf{v}}_n$ should be negative due to the topology. Bottom: An example of the event topology of reaction (3) is shown. The event is mainly triggered by the pion from the QF-Σ reaction ($|\mathbf{v}_{\mathrm{CA}} \cdot \hat{\mathbf{v}}_n| \approx 0$), while a chance to be triggered by the pion from the Λ decay ($\mathbf{v}_{\mathrm{CA}} \cdot \hat{\mathbf{v}}_n \sim$ symmetric) should be smaller.

$\lesssim p_\pi \lesssim 200$ MeV/c)? Fig. 4 (top) shows the obtained neutron momentum spectrum without $\mathbf{v}_{\mathrm{CA}} \cdot \hat{\mathbf{v}}_n$ selection. As shown, the higher momentum part looks more complicated.

Naturally, the dominant process is the kaon two-nucleon absorption followed by the hyperon decay:

$$K^- NN \rightarrow \Sigma^{\pm} n_{\Sigma\mathrm{N}} (\text{or } \ p) \quad \text{and} \quad \Sigma^{\pm} \rightarrow \pi^{\pm} n_{\Sigma\mathrm{D}}, \tag{4}$$

where $n_{\Sigma\mathrm{N}}$ is the neutron at the primary reaction and $n_{\Sigma\mathrm{D}}$ is that after $\Sigma^{\pm}$ decay. This is the event depicted in Fig.5. The $n_{\Sigma\mathrm{N}}$ should have a nature very

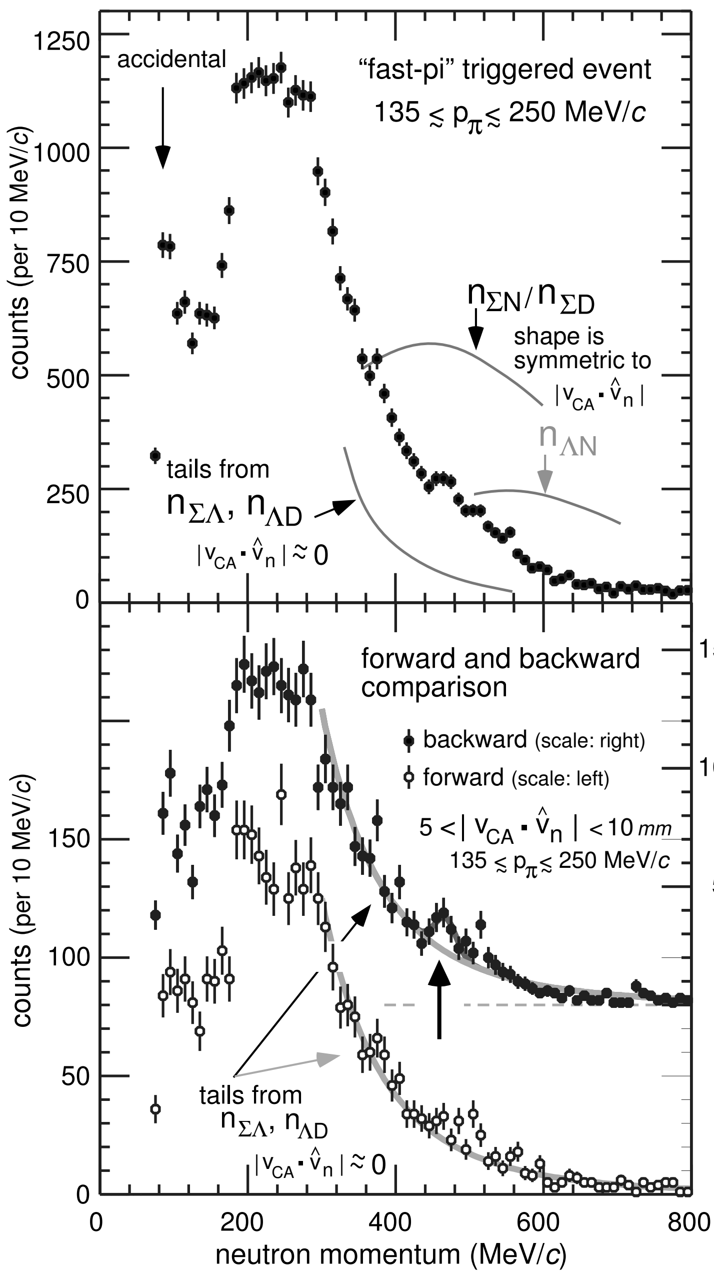

Fig. 4. Top: The neutron momentum spectrum measured in coincidence with a higher-momentum pion ($135 \lesssim p_\pi \lesssim 250$ MeV/c). Bottom: "backward" events (filled circles) ($-10mm < \mathbf{v}_{\mathrm{CA}} \cdot \hat{\mathbf{v}}_n < -5mm$) and "forward" events (open circles) ($5mm < \mathbf{v}_{\mathrm{CA}} \cdot \hat{\mathbf{v}}_n < 10mm$) are selected and compared.

similar to the $n_{\Lambda\mathrm{N}}$ in reaction (2), but shifted by $\sim$100 MeV/c to the lower side. Therefore, a "plateau" at $\sim$500 MeV/c is expected, and $\mathbf{v}_{\mathrm{CA}} \cdot \hat{\mathbf{v}}_n$ should be negative. The shape of $n_{\Sigma\mathrm{D}}$ should be nearly identical to that of $n_{\Sigma\mathrm{N}}$, since the momenta of $\Sigma^{\pm}$ and $n_{\Sigma\mathrm{N}}$ are almost equal and we detect decay pions in the 90° direction, which constrains the momentum change to be small. However, its $\mathbf{v}_{\mathrm{CA}} \cdot \hat{\mathbf{v}}_n$ should be positive.

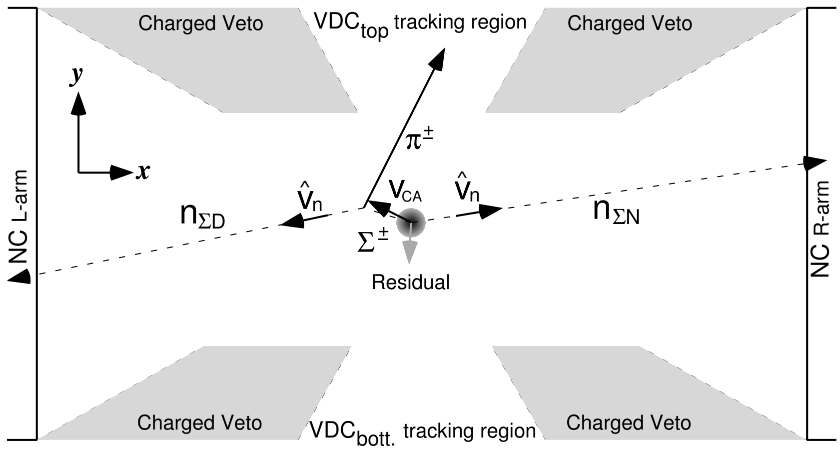

Fig. 5. An example of the event topology of the reaction 3 is shown. A scalar product $\mathbf{v}_{\rm CA} \cdot \hat{\mathbf{v}}_n$ is negative if $n_{\Sigma \rm N}$ is detected by the neutron counter, while it is positive if $n_{\Sigma D}$ is detected.

Thus, if we were to apply the same "forward-backward" decomposition to the neutron spectrum measured in coincidence with fast pions, we expect $n_{\Sigma \rm D}$ to appear in the "forward" spectrum, $n_{\Sigma \rm N}$ to appear in the "backward" spectrum, both having the same shape. The results are shown in Fig. 4 (bottom). Here we applied a relatively narrow window of $5 < |\mathbf{v}_{\rm CA} \cdot \mathbf{v}_n| < 10\ mm$. This is because the Σ dominantly decays in short distance so that the maximum asymmetry should be observed in a short range. The comparison of the two spectra reveals a peak-like enhancement at ~ 470 MeV/c in the "backward" spectrum. We assumed that the background shape of the "backward" spectrum can be inferred from that of the "forward" spectrum (as discussed above), and fitted the latter with a smooth function (shown by the grey curve). We then overlaid the same curve on top of the "backward" spectrum (also shown by the grey curve), which fairly well represents the data, except for the ~ 470 MeV/c region.

In order to test its statistical significance, we fitted the "peak" region using a Gaussian function. Although the actual functional form of the peak should be quite involved, we adopted the Gaussian form because the statistics of the peak structure does not stand for sophisticated fitting function. The excess is evaluated to be 3.6 σ, and the binding energy and the width are obtained to be $B_{Kppn} = 173 \pm 4$ MeV (measured from $K^-ppn = 3309.8$ MeV) and $\Gamma_{Kppn} < 25$ MeV, obtained by observed width of $\Gamma_{obs} = 14 \pm 4$ MeV and the experimental resolution of 6 MeV (σ @ $B = 170$ MeV).

Lets discuss what we can expect if the peak at $\sim$470 MeV/c is the signal for a bound state. If the intermediate state K^-ppn is really formed with such a large binding energy, then it should be boosted strongly opposite to the "Auger" neutron. It should then decay dominantly to ΣNN rather than ΛNN, since we observe the enhancement only in Fig. 4. The calculated momentum of decay

$\Sigma^{\pm}$ is distributed around 450 MeV/c in the backward direction and around 80 MeV/c in forward. Thus, $\mathbf{v}_{\rm CA} \cdot \hat{\mathbf{v}}_n$ for such events should be dominantly in the negative side. If there is a strongly bound $K^- ppn$ state which decays dominantly to ΣNN, we expect that: i) the signal is enhanced by the $\mathbf{v}_{\rm CA} \cdot \hat{\mathbf{v}}_n$ selection, and ii) the enhancement is in the negative $\mathbf{v}_{\rm CA} \cdot \hat{\mathbf{v}}_n$ side. The enhancement observed in the "backward" spectrum of Fig. 4 does satisfy these criteria, and is statistically significant (3.6σ). It is not an artifact of reduced statistics, introduced by the rather tight cut on $\mathbf{v}_{\rm CA} \cdot \hat{\mathbf{v}}_n$, since the structure is already visible in the high-statistics "fast-pi" spectrum before applying the $\mathbf{v}_{\rm CA} \cdot \hat{\mathbf{v}}_n$ cut.

In summary, we have found an evidence for a strongly bound kaonic system $\mathrm{K}^- ppn$, whose major decay mode is $K^- ppn \to \Sigma NN$.

The present finding shows the presence of strongly bound systems with K^- and provides important information on the KN interaction, nuclear compressibility, high-density nuclear structure and chiral symmetry restoration, which are more or less unknown as of today.

We are grateful to Y. Akaishi and R. Seki for useful discussion. We owe much for M. Iwai, K. Taniguchi, O. Sasaki, N. Kimura, M. Sekimoto and all the member of KEK-PS for their substantial cooperation. We thank IHI for collaborative development for CFRP vacuum jacket. This work is supported by MEXT, KEK, Riken, KOSEF, NSF, DOE and KRF.

References

[1] M. Iwasaki *et al.*, Phys. Rev. Lett., 78 (1997) 3067.
T.M. Ito *et al.*, Phys. Rev. C58 (1998) 2366.

[2] Y. Akaishi and T. Yamazaki, Phys. Rev., C65 (2002) 044005.

[3] A. Dote, Y. Akaishi and T. Yamazaki, Prog. Theor. Phys. Suppl., 146 (2003) 508.

[4] T. Hatsuda and T. Kunihiro, Prog. Theor. Phys., 74 (1985) 765.

[5] B. Freedman, L.D. McLerran, Phys. Rev., D17 (1978) 1109; ; G.E. Brown *et al.*. Nucl. Phys. **A567**, 937 (1994)..

[6] M. Iwasaki *et al.*, Nucl. Instrum. Meth., A473 (2001) 286.

[7] H. Outa *et al.*, Prog. Theor. Phys. Suppl., 117 (1994) 177.